O índice de refração: propriedades e técnicas de medidas

Sérgio Carlos Zilio
IFSC - USP

Roteiro

1) O índice de refração e suas propriedades

2) Técnicas de medida

   a) Refração/reflexão

   b) Interferometria/elipsometria

   c) Guias de ondas

3) Óptica não linear (franjas de Maker)

O índice de refração

v = c / n

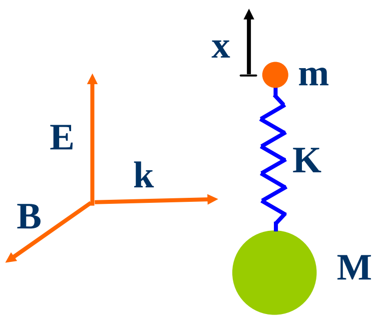

$$m\frac{d^2x}{dt^2} + mb\frac{dx}{dt} + Kx = -eE$$

$$E \sim e^{-i\omega t}$$

$$x = \frac{eE/m}{\omega_0^2 - \omega^2 - i\omega b}$$

$$P = -Nex = \varepsilon_0 \tilde{\chi}\, E$$

$$\tilde{\chi} = \frac{Ne^2/m\varepsilon_0}{\omega_0^2 - \omega^2 - i\omega b}$$

$$\tilde{n} = \sqrt{\frac{\varepsilon}{\varepsilon_0}} = \sqrt{\left(1+\tilde{\chi}\right)} \approx 1 + \frac{1}{2}\tilde{\chi} + \ldots.. = n + i\,\kappa$$

$$n = 1 + \left(\frac{Ne^2}{2m\varepsilon_0}\right)\frac{\left(\omega_0^2 - \omega^2\right)}{\left(\omega_0^2 - \omega^2\right)^2 + (\omega b)^2}$$

$$\omega = 2\pi c / \lambda$$

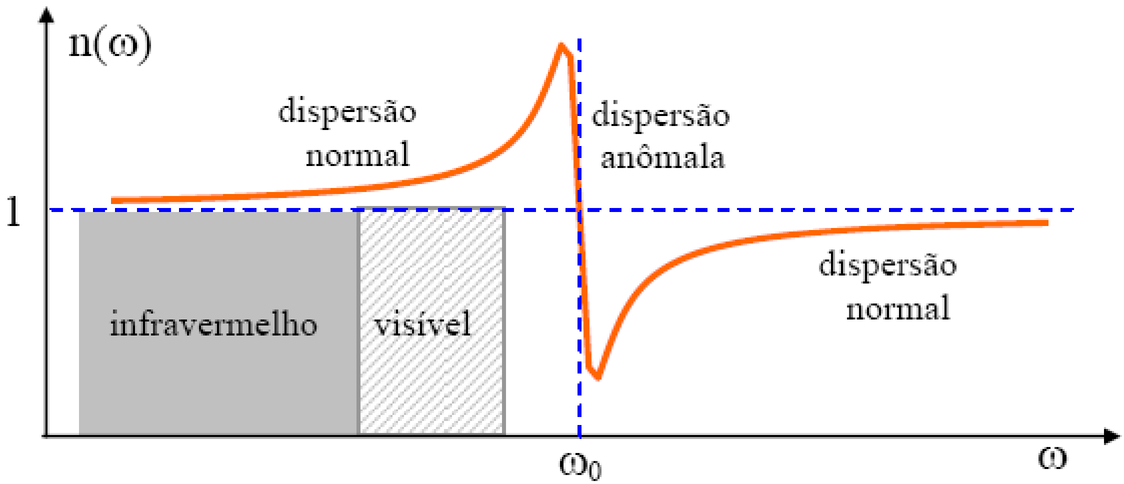

Equação de Sellmeier

$$n^2(\lambda) = 1 + \frac{B_1\lambda^2}{\lambda^2 - C_1} + \frac{B_2\lambda^2}{\lambda^2 - C_2} + \frac{B_3\lambda^2}{\lambda^2 - C_3} + ... = 1 + \sum_i \frac{B_i\lambda^2}{\lambda^2 - C_i}$$

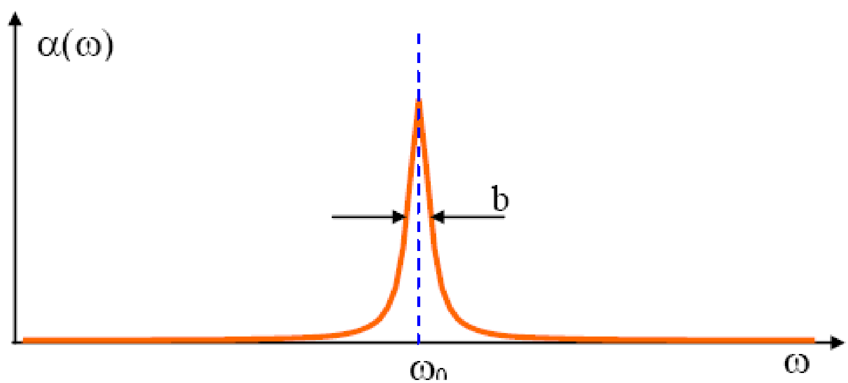

$$\alpha(\omega) = \kappa\frac{\omega}{c} = \left(\frac{Ne^2}{mc\varepsilon_0}\right)\frac{\omega^2 b}{\left(\omega_0^2 - \omega^2\right)^2 + (\omega b)^2}$$

O índice de refração

$$n_1 sen\theta_1 = n_2 sen\theta_2$$

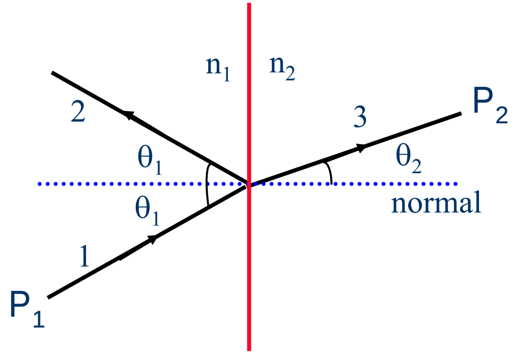

Princípio de Fermat

$$\delta \int_{P_1}^{P_2} n(s)\, ds = 0$$

Condições de contorno para E e H equações de Fresnel

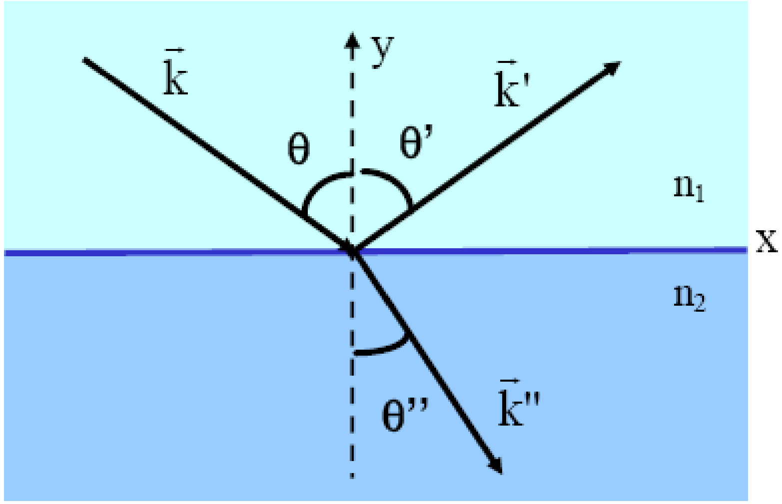

Propriedades do índice de refração

$n = n(\lambda)$	dispersão	decomposição espectral da luz, GVD
$n = n(\vec{r})$	não homogeneidade	trajetória não retilínea $\frac{d}{ds}\left(n\frac{d\vec{r}}{ds}\right) = \vec{\nabla}n$
$n_x \neq n_y$	anisotropia	birrefringência, dicroismo se $\alpha_x \neq \alpha_y$
$n_+ \neq n_-$	meios chirais	atividade óptica
$n = n(T)$	efeito termo-óptico	lente térmica
$n = n(E)$	efeito eletro-óptico	moduladores de luz, geração de novas frequências, birrefringência induzida
$n = n(B)$	efeito Faraday	isoladores ópticos
$n = n(I)$	auto-modulação de fase - efeito Kerr óptico	chaves ultra-rápidas
$n = n(\sigma)$	efeito foto-elástico	moduladores acusto-ópticos

2) Técnicas de medida

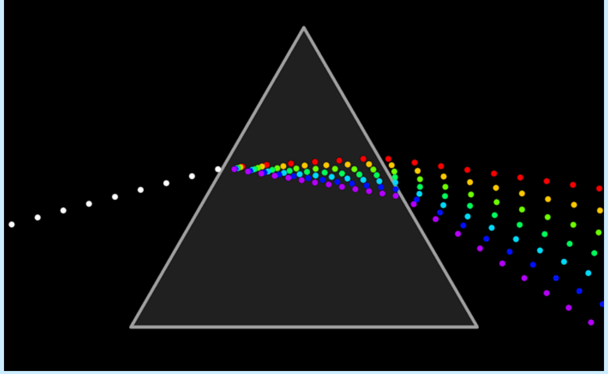

a)Refração/reflexão

(i) Método do ângulo de desvio mínimo

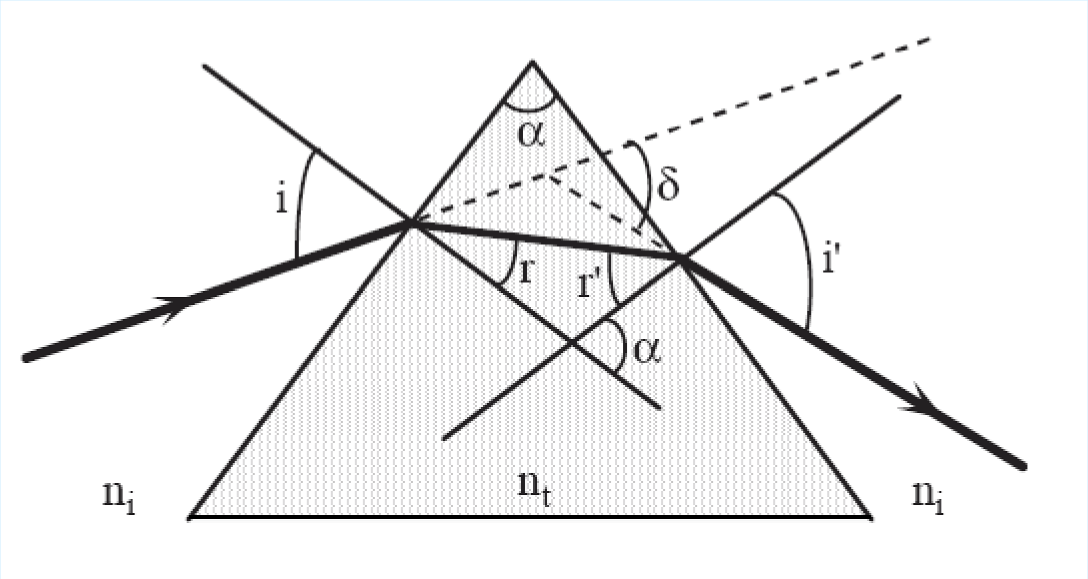

$$n(\lambda) = \frac{\sin\left(\frac{\delta_m(\lambda)+\alpha}{2}\right)}{\sin\left(\frac{\alpha}{2}\right)} n_i(\lambda)$$

Tipicamente, para se obter uma incerteza do índice da ordem de 10^{-5}, requer-se uma incerteza angular menor que 1″

Precisão típica: 10^{-4} a 10^{-5}

Absolute refractive indices and thermal coefficients of fused silica and calcium fluoride near 193 nm

Rajeev Gupta, John H. Burnett, Ulf Griesmann, and Matthew Walhout

APPLIED OPTICS / Vol. 37, No. 25 / 1 September 1998

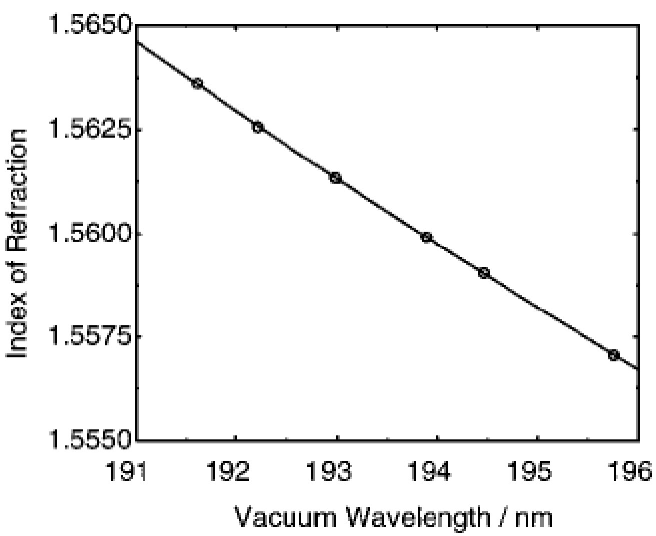

Table 4. Uncertainty Budget of Refractive-Index Measurements

Source of Uncertainty	Value	Index uncertainty
Apex angle measurement	0.24″	0.8×10^{-6}
Wild spectrometer measurement		
Temperature uncertainty	0.12 °C	1.5×10^{-6}
Deviation measurement uncertainty	1.1″	3.6×10^{-6}
Gaertner spectrometer measurement		
Temperature uncertainty	0.07 °C	1.4×10^{-6}
Deviation measurement uncertainty	1.9″	5.9×10^{-6}
Refractive index of air		
Index uncertainty in DUV		0.2×10^{-6}
Barometric pressure variation		7.0×10^{-6}
Humidity variation		0.2×10^{-6}
Combined index uncertainty (1σ)		10.1×10^{-6}

Absolute refractive indices and thermal coefficients of CaF_2, SrF_2, BaF_2, and LiF near 157 nm

John H. Burnett, Rajeev Gupta, and Ulf Griesmann

APPLIED OPTICS / Vol. 41, No. 13 / 1 May 2002

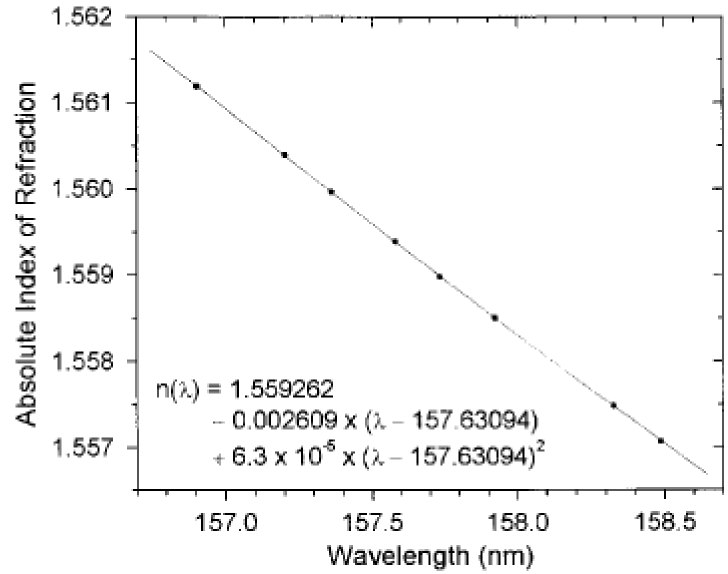

Table 2. Uncertainty Budget for Refractive-Index Measurement

Source of Uncertainty	Value	Index Uncertainty
Apex angle A	0.24 arc sec	0.7×10^{-6}
Deviation angle D		
Visible goniometer deviation measurement uncertainty	1.1 arc sec	
Visible goniometer effect of temp., press., hum. uncertainty	0.1 arc sec	
UV goniometer deviation measurement uncertainty	1.2 arc sec	
Net deviation angle uncertainty	1.63 arc sec	4.9×10^{-6}
Wavelength λ	0.02 pm	0.1×10^{-6}
Index of N_2 gas n_{gas}		
Index uncertainty	0.2×10^{-6}	0.2×10^{-6}
Temperature uncertainty	0.05 °C	0.1×10^{-6}
Pressure uncertainty	1 bar	0.3×10^{-6}
Material temperature	0.05°	0.3×10^{-6}
Correction to 20 °C	0.05	0.6×10^{-6}
Intrinsic birefringence	$1(3) \times 10^{-6}$	$1(3) \times 10^{-6}$
Combined uncertainty[a]		$5.1(5.8) \times 10^{-6}$

[a]All uncertainties are standard ($k = 1$) uncertainties.

ii) Refratômetro de Abbe

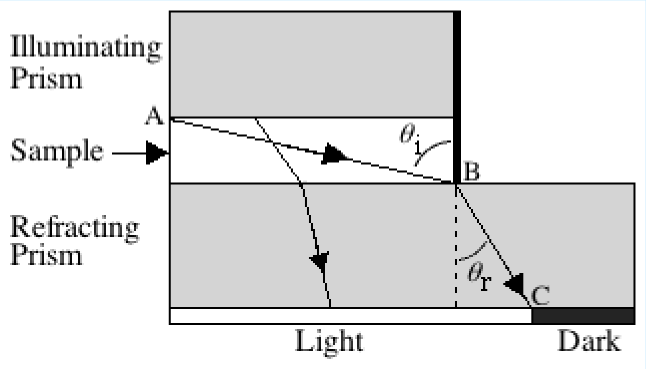

Precisão típica: 10^{-3} a 10^{-4}

iii) Refratômetro de Pulfrich

Precisão típica: 10^{-4} a 10^{-5}

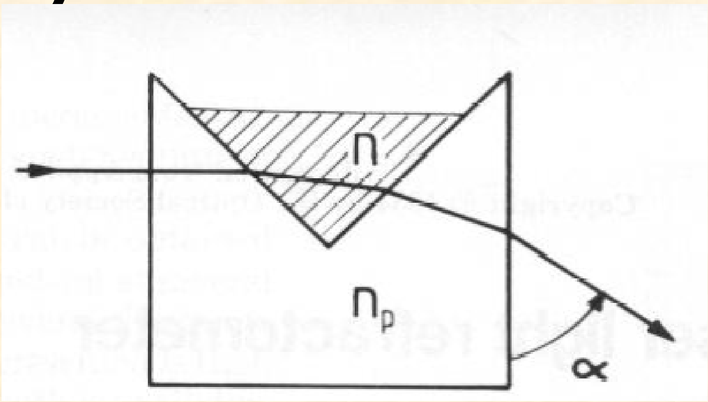

$$n = \sqrt{n_p^2 - \cos\alpha\sqrt{n_p^2 - \cos^2\alpha}}$$

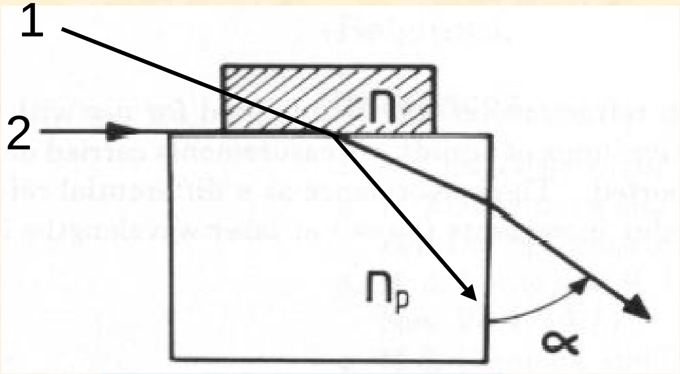

$$n = \sqrt{n_p^2 - \cos^2\alpha}$$

b) Interferometria

i) Múltiplos feixes

$$I(\delta) = \frac{I_0}{1 + F\,\mathrm{sen}^2\delta}$$

$$\delta = \frac{2\pi}{\lambda_0} nt$$

$$F = 4R/(1-R)^2$$

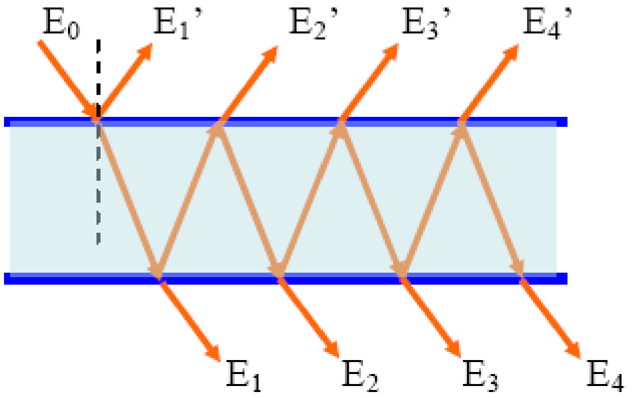

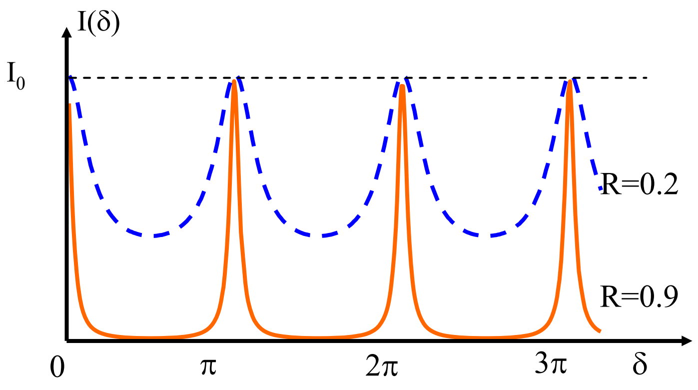

High accuracy ultraviolet index of refraction measurements using a Fourier transform spectrometer

Rajeev Gupta and Simon G. Kaplan

[J. Res. Natl. Inst. Stand. Technol. **108**, 429-437 (2003)]

$$\delta_{max} = \frac{2\pi}{\lambda_m} nt = \pi m$$

$$\lambda_m = \frac{2n(\nu)t}{\pi m}$$

$$I(\delta) = \frac{I_0}{1 + F\,sen^2\delta} \approx I_0 (1 - F\,sen^2\delta)$$

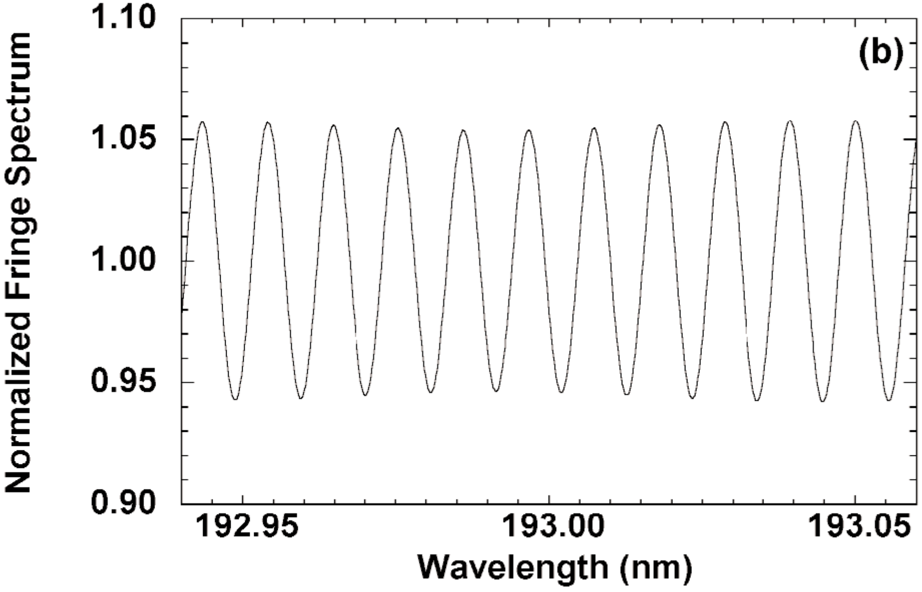

Table 1. Uncertainty budget for index of refraction measurement of 1 mm thick CaF_2 etalon sample at 193 nm

Uncertainty Source	Type	Standard uncertainty	Rel. std uncertainty in *n*
Thickness measurement (nm)	B	6	5.83E–06
Angle of incidence (°)	B	0.12	2.19E–06
Beam divergence (°)	B	0.15	4.00E–07
Temperature (K)	B	0.5	5.75E–06
Wavenumber error in UV-FTS (cm^{-1})	B	0.1	1.93E–06
Peak center determination (cm^{-1})	A	0.02	3.86E–07
Fringe order	B	0	0.00E+00
Intrinsic birefringence (10^{-6})	B	0.34	3.40E–07
Quadrature Sum			8.72E–06
Uncertainty in *n* ($k = 1$)		1.31E-05	

Refractometer for tracking changes in the refractive index of air near 780 nm

N. Khélifa, H. Fang, J. Xu, P. Juncar, and M. Himbert

APPLIED OPTICS / Vol. 37, No. 1 / 1 January 1998

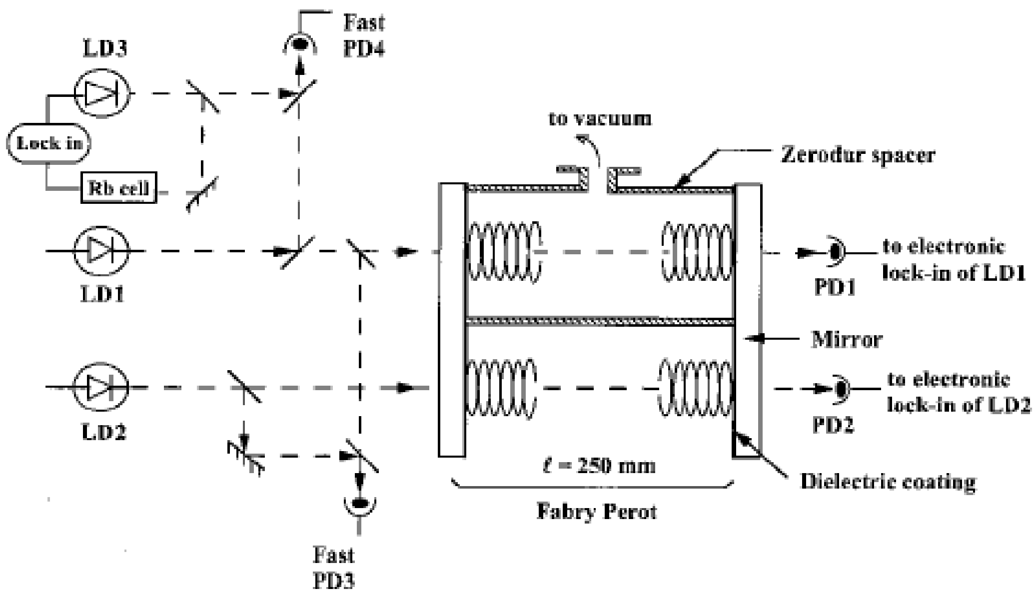

The relative uncertainty of our measurements reaches the level 2 x 10^{-8}.

ii) Elipsometria

A elipsometria é sensível a diversas características dos materiais, tais como espessura da camada, constantes óticas (índice de refração e coeficiente da extinção), rugosidade da superfície, composição e anisotropia ótica

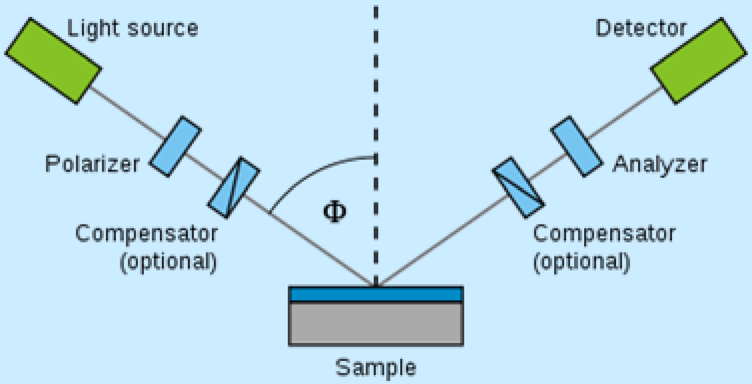

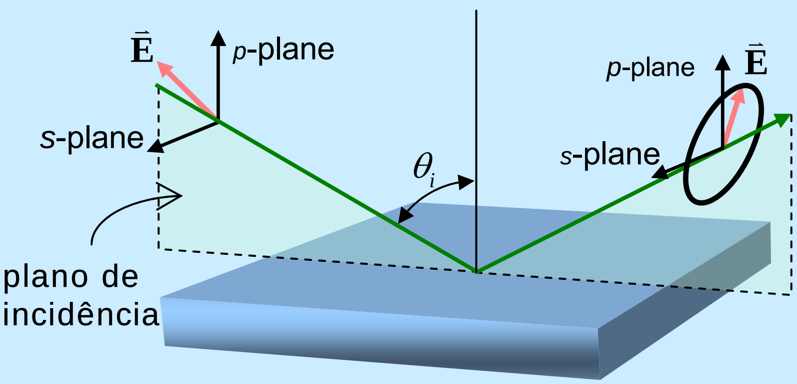

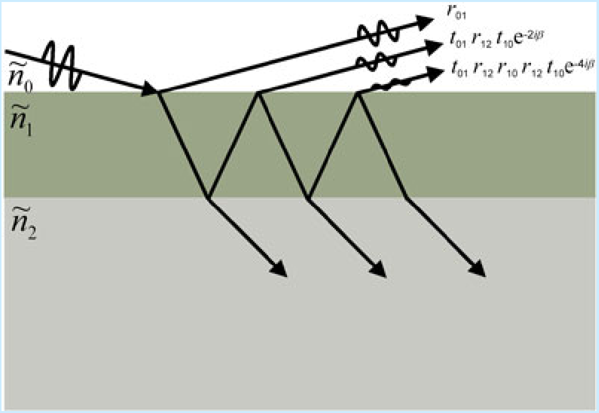

iii) Dois feixes (Michelson)

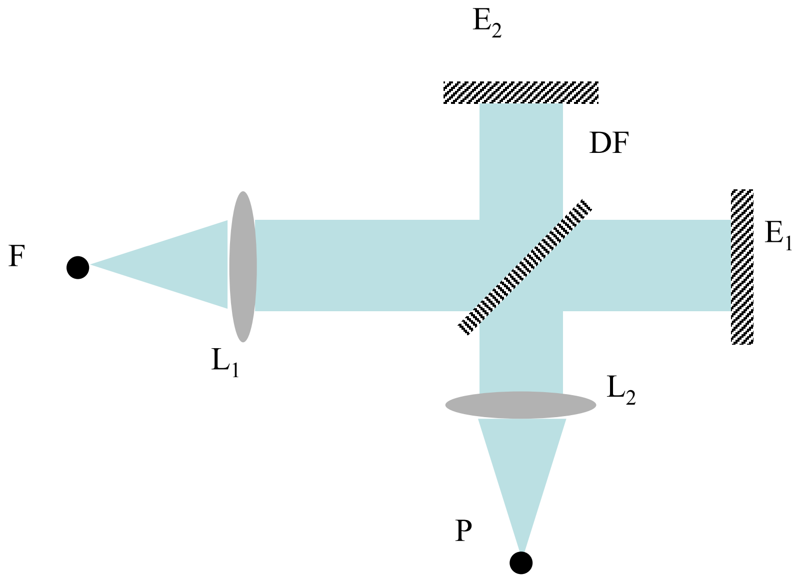

$$I(\Delta) = I_F \left[1 + \cos\left(\frac{2\pi}{\lambda_0} \Delta \right) \right]$$

$$\Delta = nd$$

High-accuracy interferometer with a prism pair for measurement of the absolute refractive index of glass

Yasuaki Hori,* Akiko Hirai, Kaoru Minoshima, and Hirokazu Matsumoto

10 April 2009 / Vol. 48, No. 11 / APPLIED OPTICS

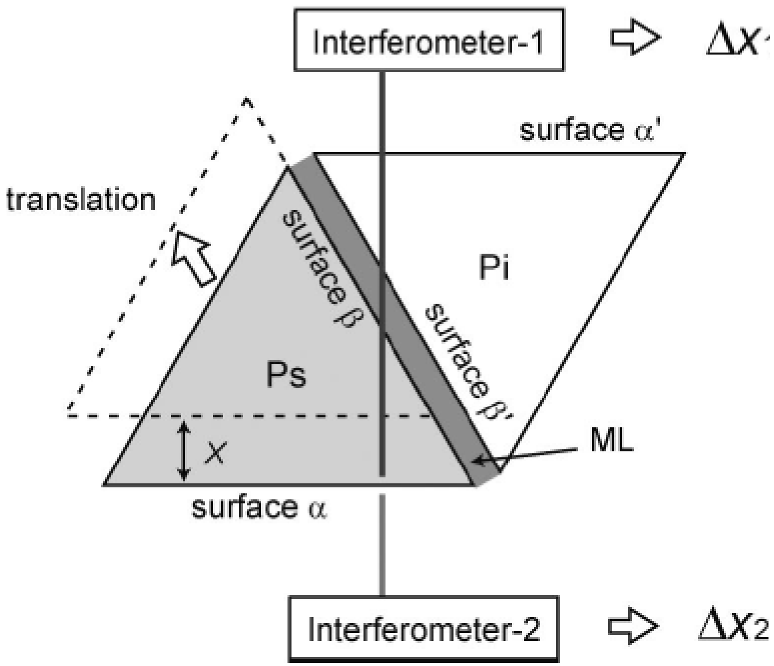

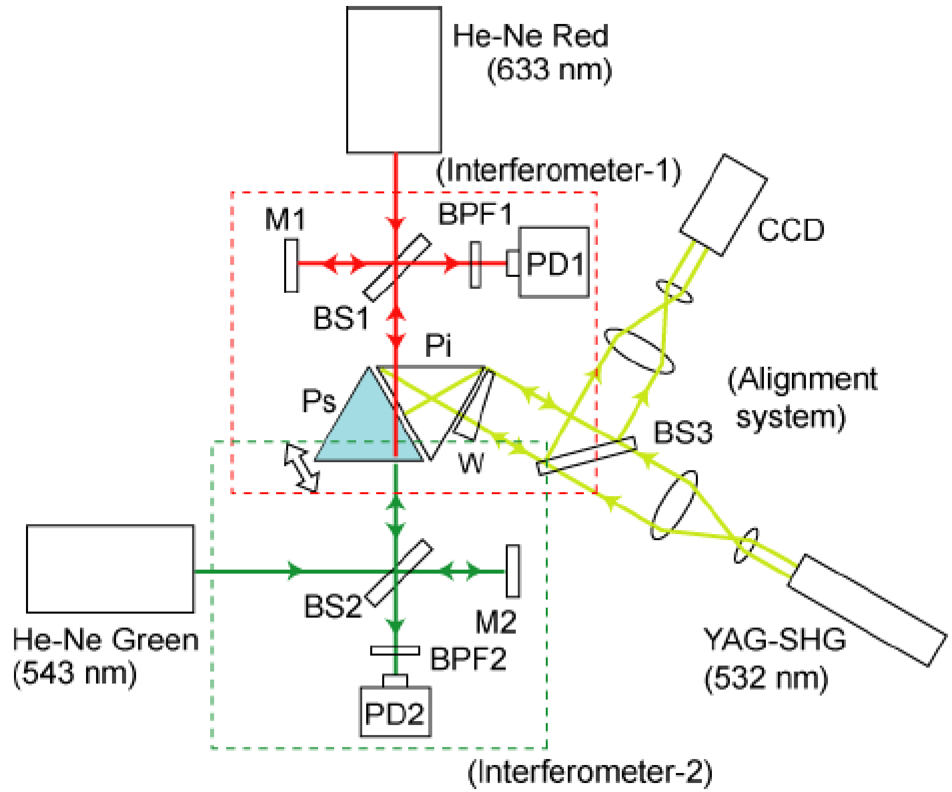

Table 1. Uncertainty Budget of the Proposed Method[a]

Category	Factor x_i	$u(x_i)$	$\partial f/\partial x_i$	Uncertainty u_i
Interferometer	Wavelength (633 nm)	$3.8 \times 10^{-9}\,\mu$m	n_s/λ_2	9.1×10^{-9}
	Wavelength (543 nm)	$3.1 \times 10^{-7}\,\mu$m	$n_s\lambda_1/\lambda_2{}^2$	8.6×10^{-7}
	Phase measurement of interferometer 1	0.16 rad	$\lambda_1/4\pi\Delta x_2$	(9.5×10^{-7}) [b]
	Alignment of interferometer 1	2.3×10^{-4} rad	$(n_s/6) \times u(\theta_1)$ [c]	1.3×10^{-8}
	Phase measurement of interferometer 2	0.16 rad	$n_s\lambda_2/4\pi\Delta x_2$	(1.2×10^{-6}) [b]
	Alignment of interferometer 2	4.3×10^{-4} rad	$(n_s/6) \times u(\theta_2)$ [c]	4.7×10^{-8}
	Alignment between prism and stage	$0.038\,\mu$m	$(n_s - n_L)/\Delta x_2 \cos\theta_a$	2.5×10^{-7}
	Abbe's error (yawing, pitching)	1.0×10^{-5} rad	$n_s\Delta d/\Delta x_2$	8.7×10^{-7}
Measurement	Repeatability	$1.91 \times 10^{-6}/\sqrt{10}$	1	6.0×10^{-7}
	Drift	4.3×10^{-7}	1	4.3×10^{-7}
	Sample setting	negligible	1	negligible
	Movement of incident prism	$1.9 \times 10^{-3}\,\mu$m	$1/\Delta x_2$	2.2×10^{-7}
Refractive index of air	Temperature measurement of air	20 mK	$n_s(dn_a/dT)$	2.8×10^{-8}
	Pressure measurement of air	0.05 hPa	$n_s(dn_a/dP)$	2.0×10^{-8}
Sample under measurement	Temperature measurement of sample	20 mK	dn/dT	5.8×10^{-8}
	Flatness of sample	$\lambda/10\,\mu$m	$(n_s - n_L)/\Delta x_2 \cos\theta_a$	4.0×10^{-7}
	Homogeneity of sample	5.8×10^{-7}	1	5.8×10^{-7}
		Combined standard uncertainty		1.6×10^{-6}
		Expanded uncertainty ($k = 2$)		3.3×10^{-6}

Self-referenced spectral interferometry for simultaneous measurements of thickness and refractive index

Jihoon Na,[1] Hae Young Choi,[1] Eun Seo Choi,[2] ChangSu Lee,[3] and Byeong Ha Lee[1,*]

1 May 2009 / Vol. 48, No. 13 / APPLIED OPTICS

$$I(\sigma) = I_0(\sigma)\int f(\Delta)\cos(2\pi\sigma\Delta)\,d\Delta \qquad \sigma = 1/\lambda$$

$$t = \Delta\ell - \Delta,$$

$$n_g = \Delta\ell / t.$$

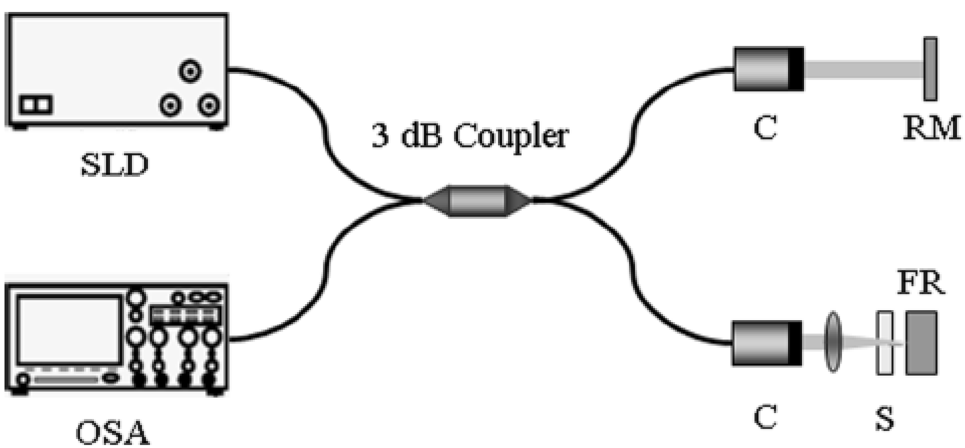

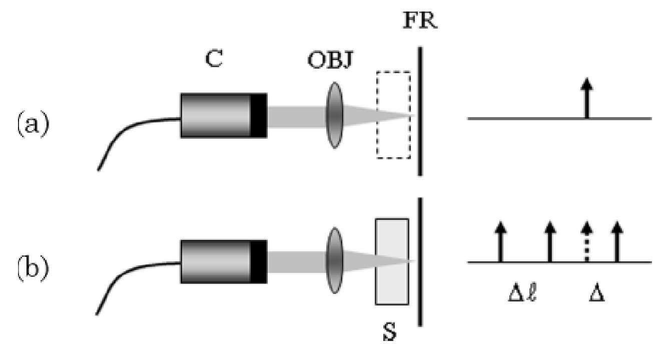

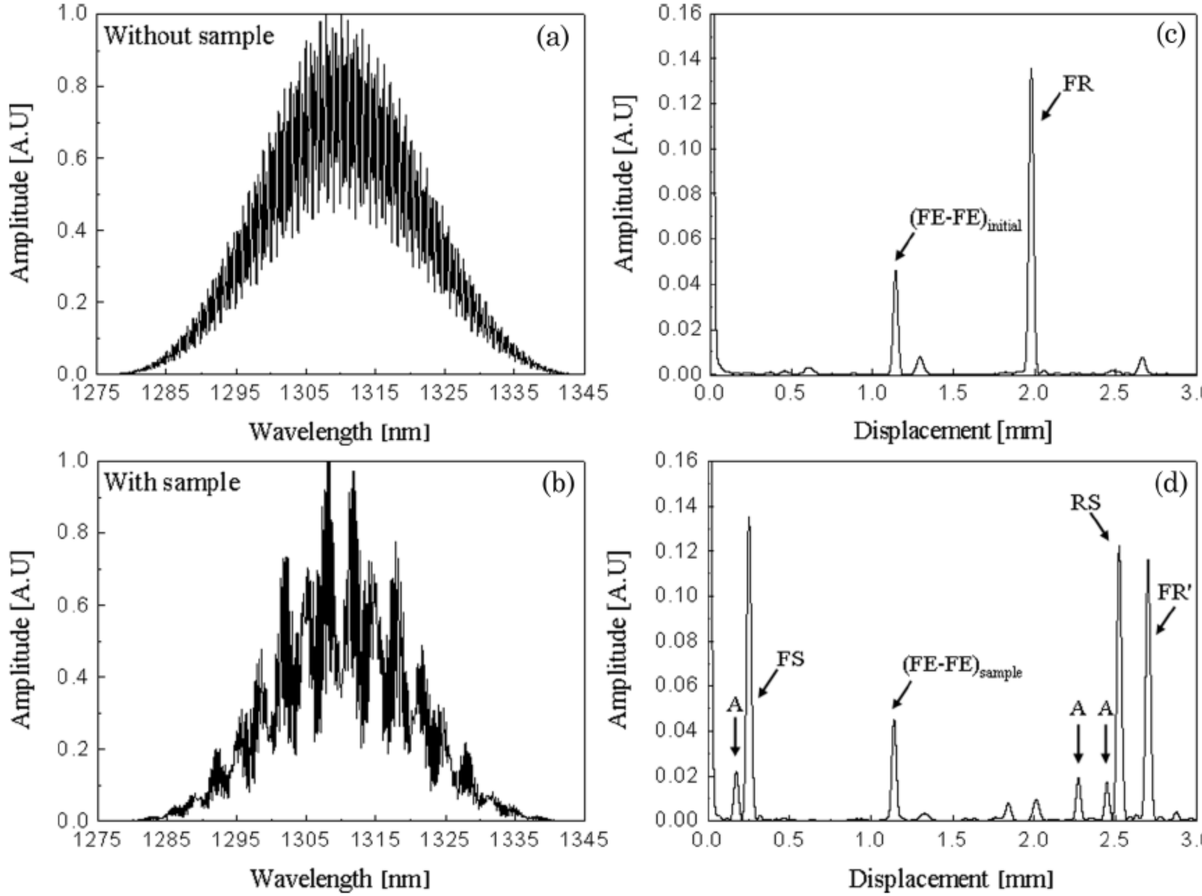
Without sample
(a)
Amplitude [A.U]
Wavelength [nm]
(c)
FR
(FE-FE)initial
Amplitude [A.U]
Displacement [mm]
With sample
(b)
Amplitude [A.U]
Wavelength [nm]
(d)
RS
FR'
FS
(FE-FE)sample
A
A
A
Amplitude [A.U]
Displacement [mm]

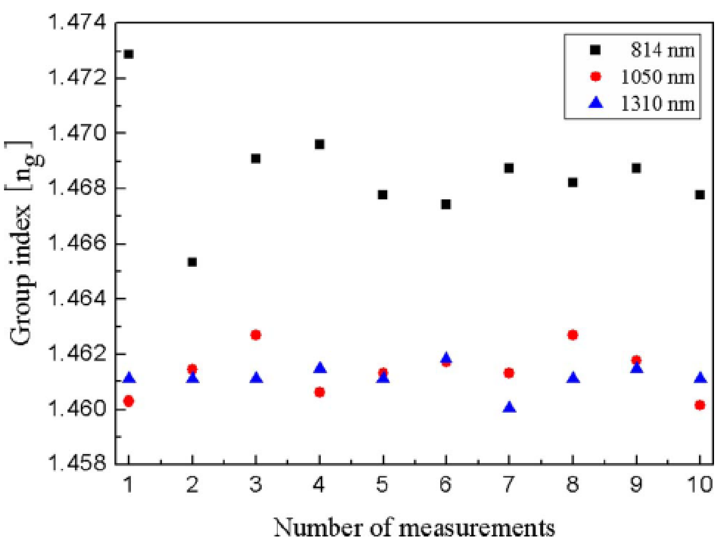

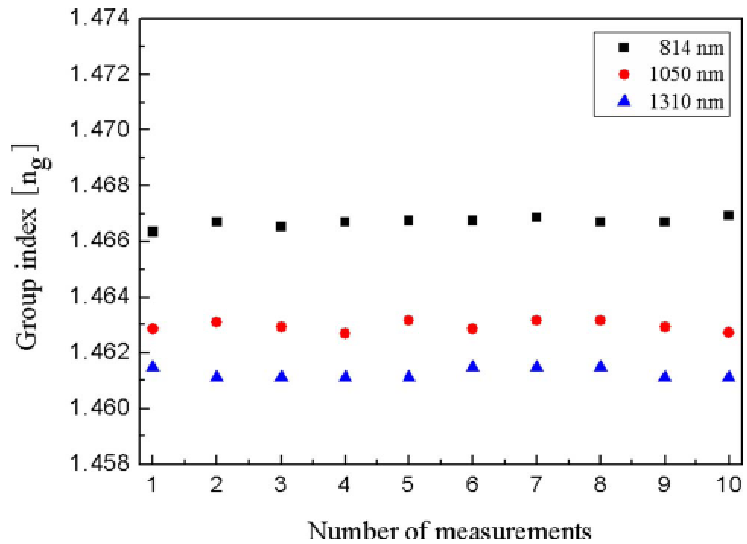

		Group Index (n_g)			Thickness (mm)		
Sample	Wavelength [nm]	Reference	Measurements	Self-Referenced Measurements	Reference	Measurements	Self-Referenced Measurements
Fused Silica	814	1.4667	1.4686 ± 0.0019	1.4667 ± 0.0002	—	1.5526 ± 0.0020	1.5546 ± 0.0002
	1050	1.4625	1.4614 ± 0.0009	1.4629 ± 0.0002	1.555	1.5563 ± 0.0010	1.5546 ± 0.0002
	1310	1.4616	1.4612 ± 0.0005	1.4613 ± 0.0002	—	1.5557 ± 0.0005	1.5556 ± 0.0002

c) Guias de ondas

i) Fibras ópticas

Redes de período longo (LPG)

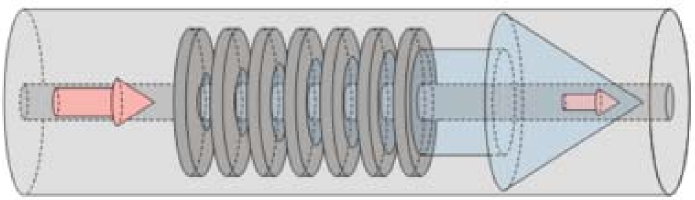

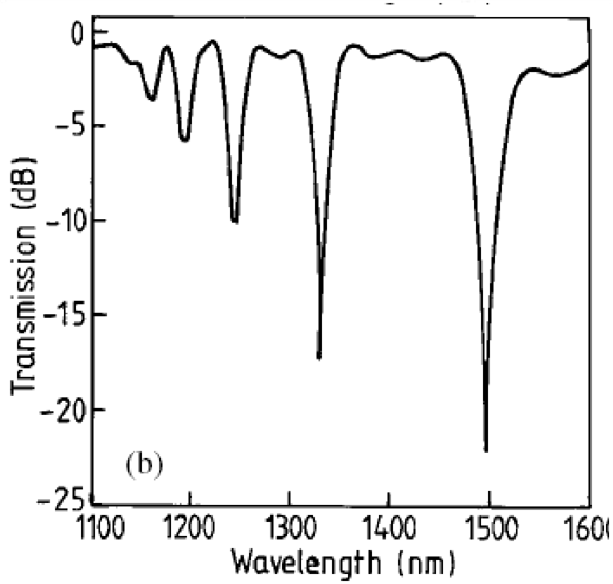

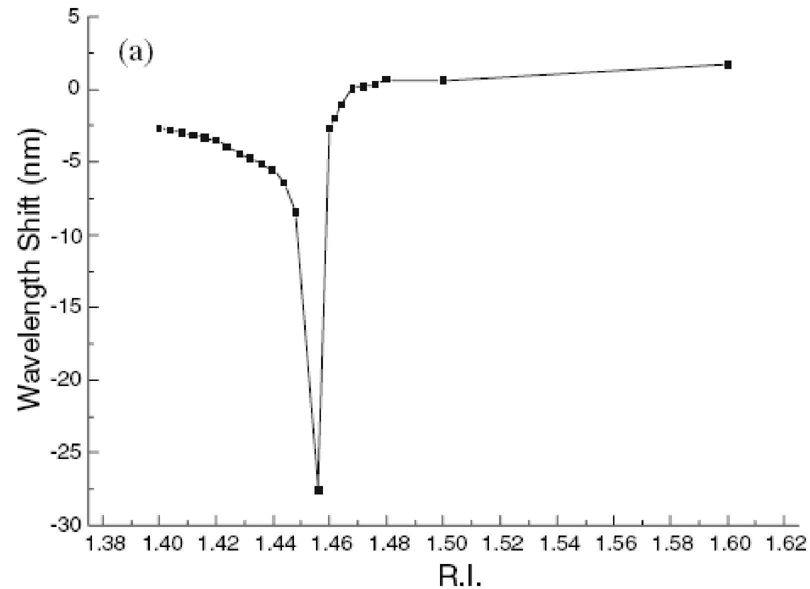

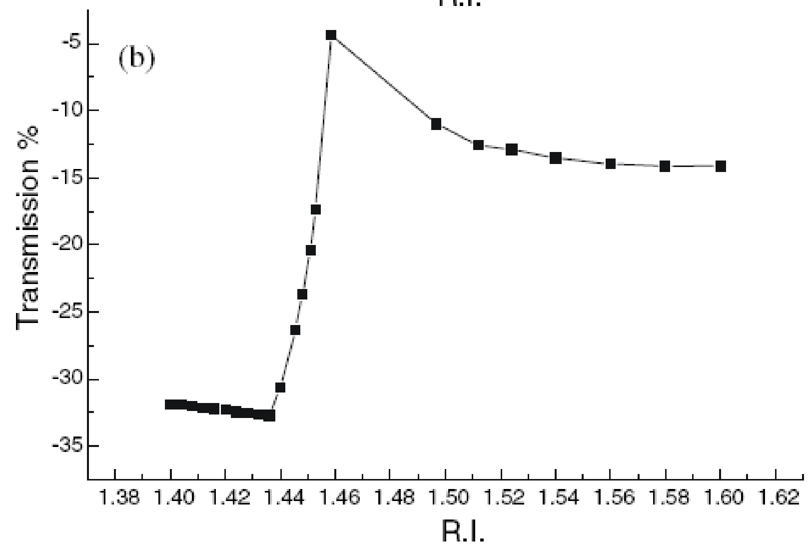

Redes de Bragg inclinadas (TFBG)

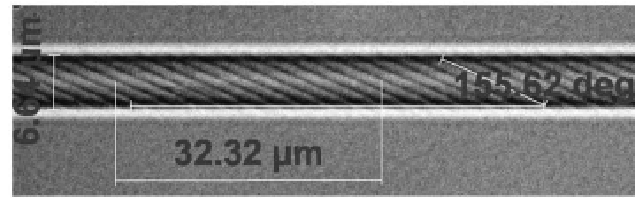

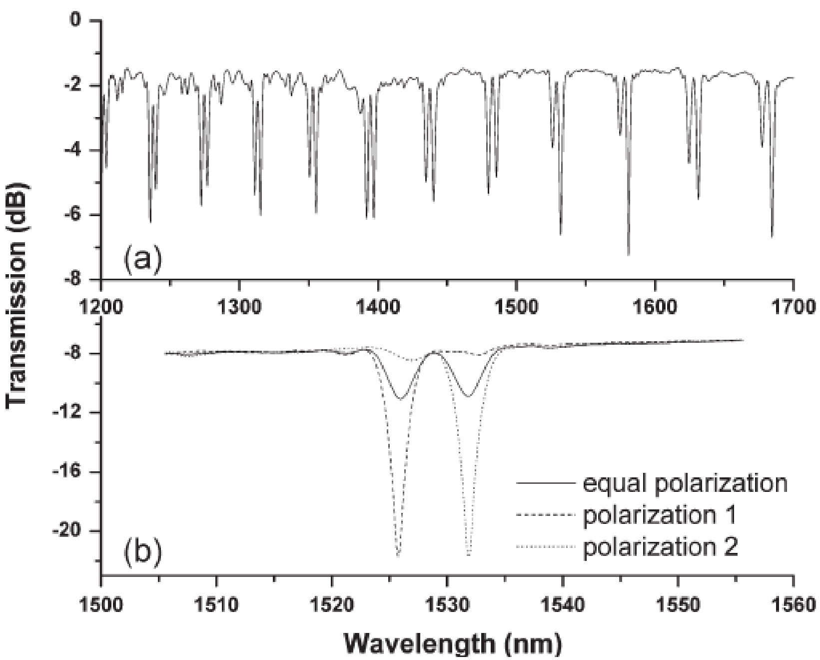

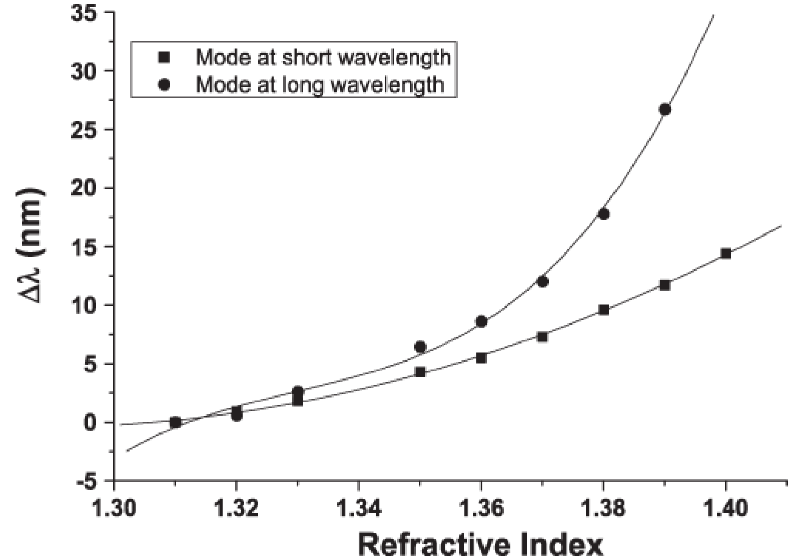

ii) Guias planares

Plasmons de superfície

Plasmons: oscilações coletivas da densidade de um gás de elétrons livres, freqüentemente ocorrendo em freqüências óticas.

Plasmons de superfície: plasmons confinados à superfície (interface) e interagem com a luz, resultando em polaritons.

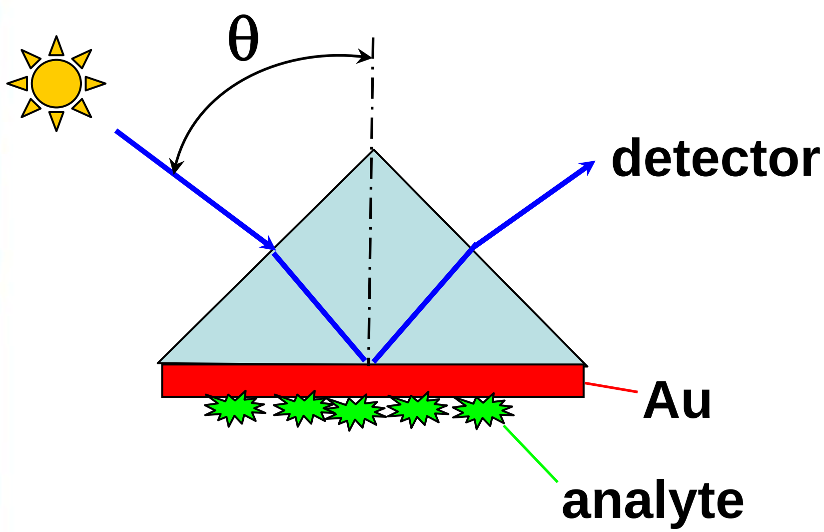

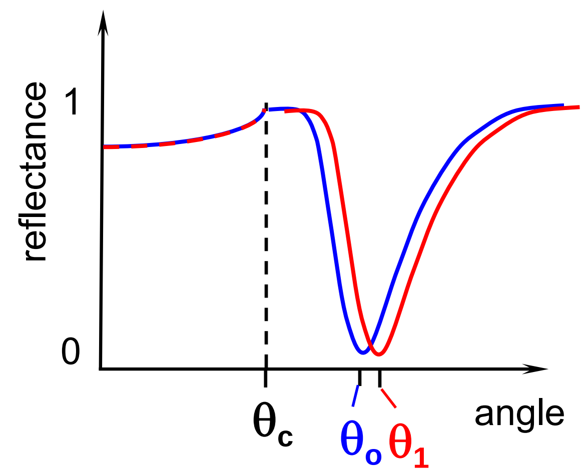

Tipos de acoplamento

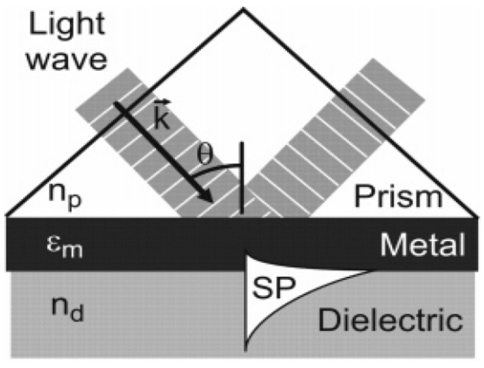

Prism coupler (Kretschmann)

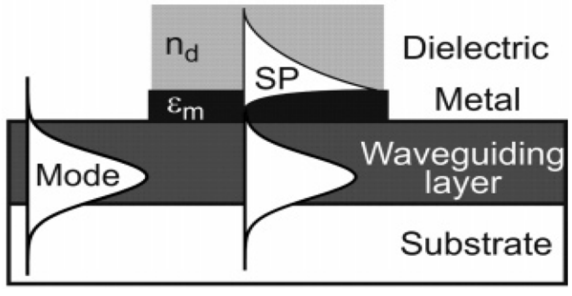

Waveguide coupler

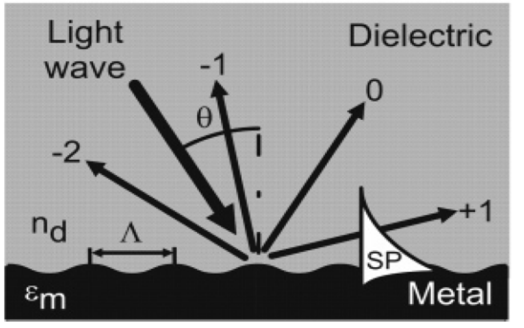

Grating coupler

Precisão típica: 10^{-5}

Guias dielétricos

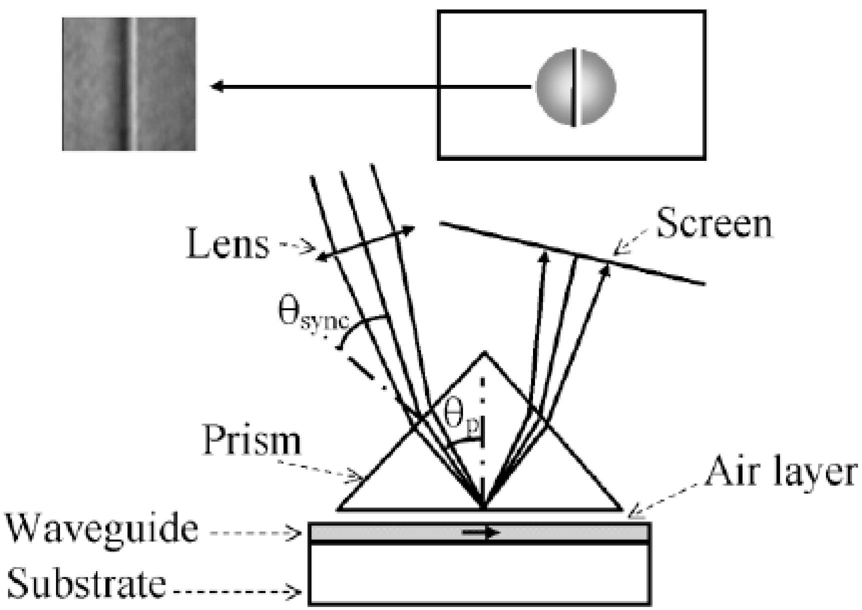

$$2d_3 \frac{\omega}{c} n_3 \cos\theta_3 = \psi_{34} + \psi_{321} + 2m\pi \ ,$$

$$m = 0,\ 1,\ 2,\ \ldots\ .$$

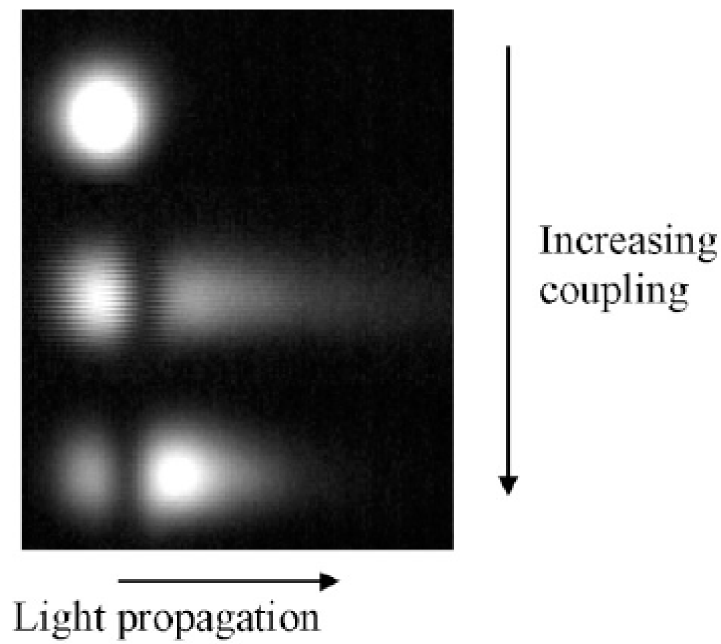

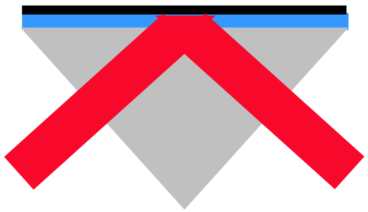

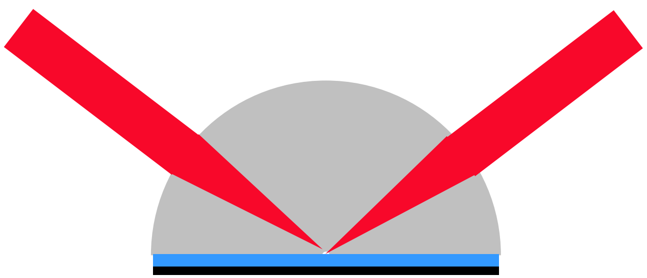

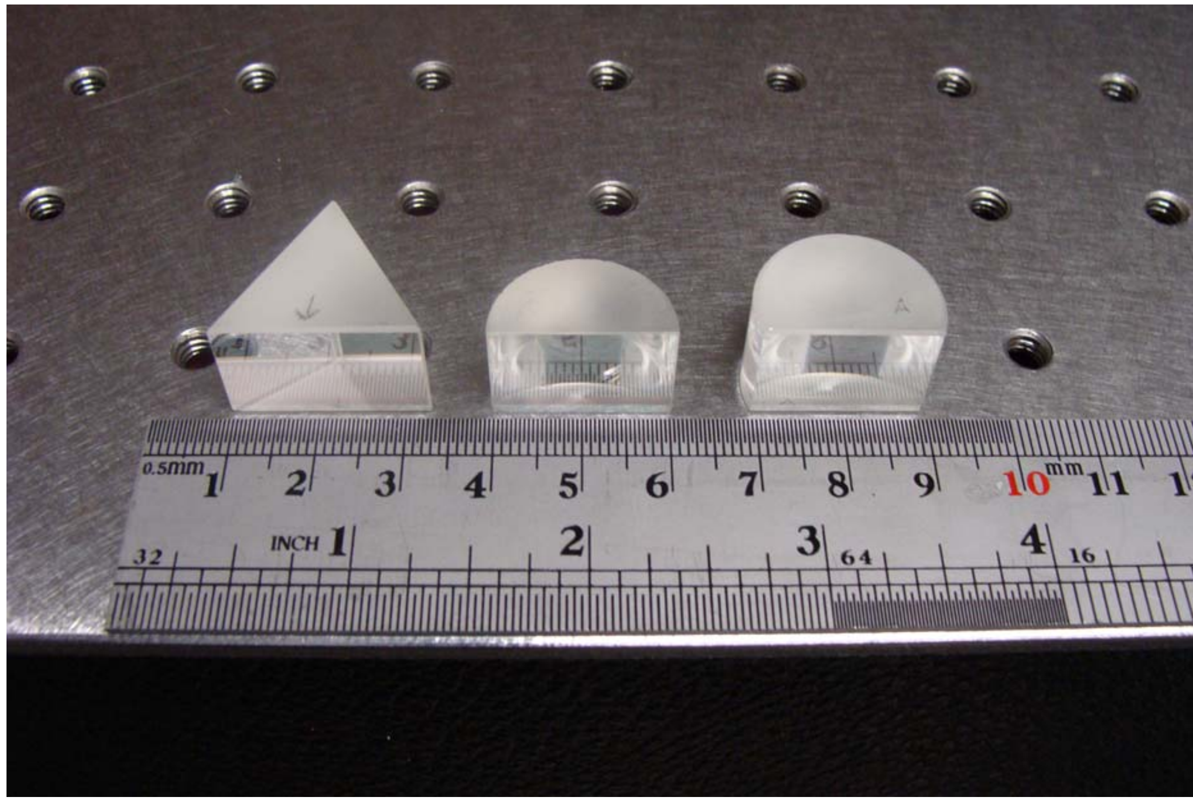
0.5mm
INCH

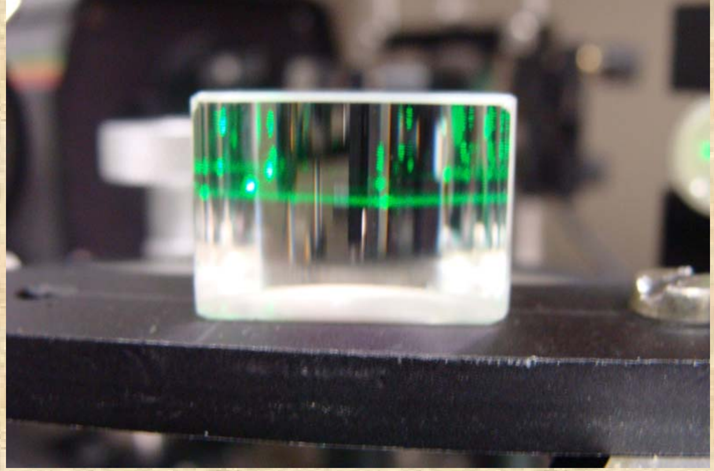

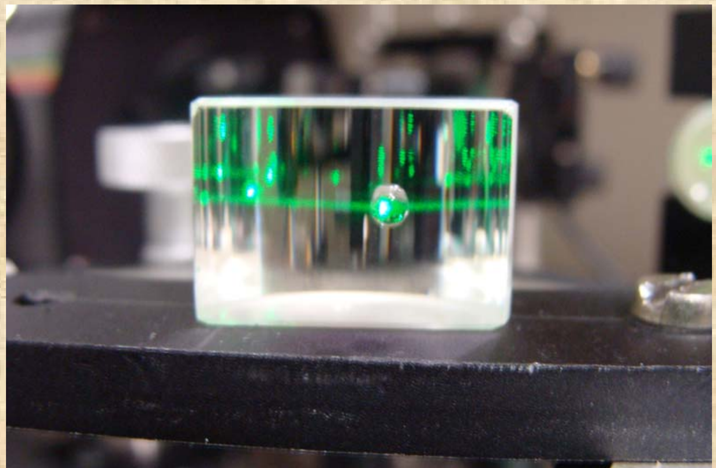

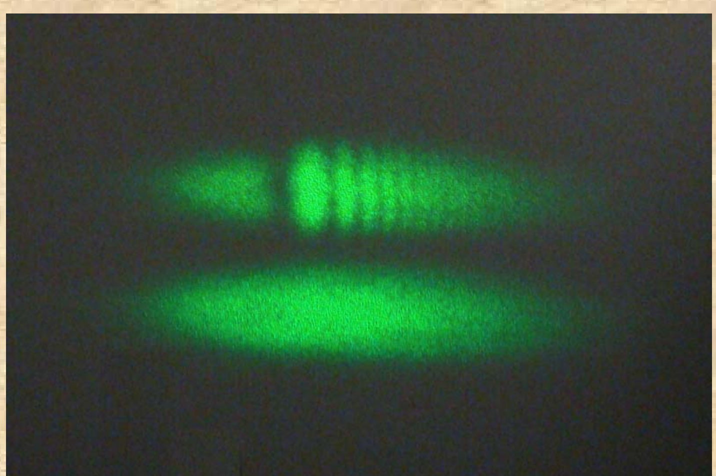

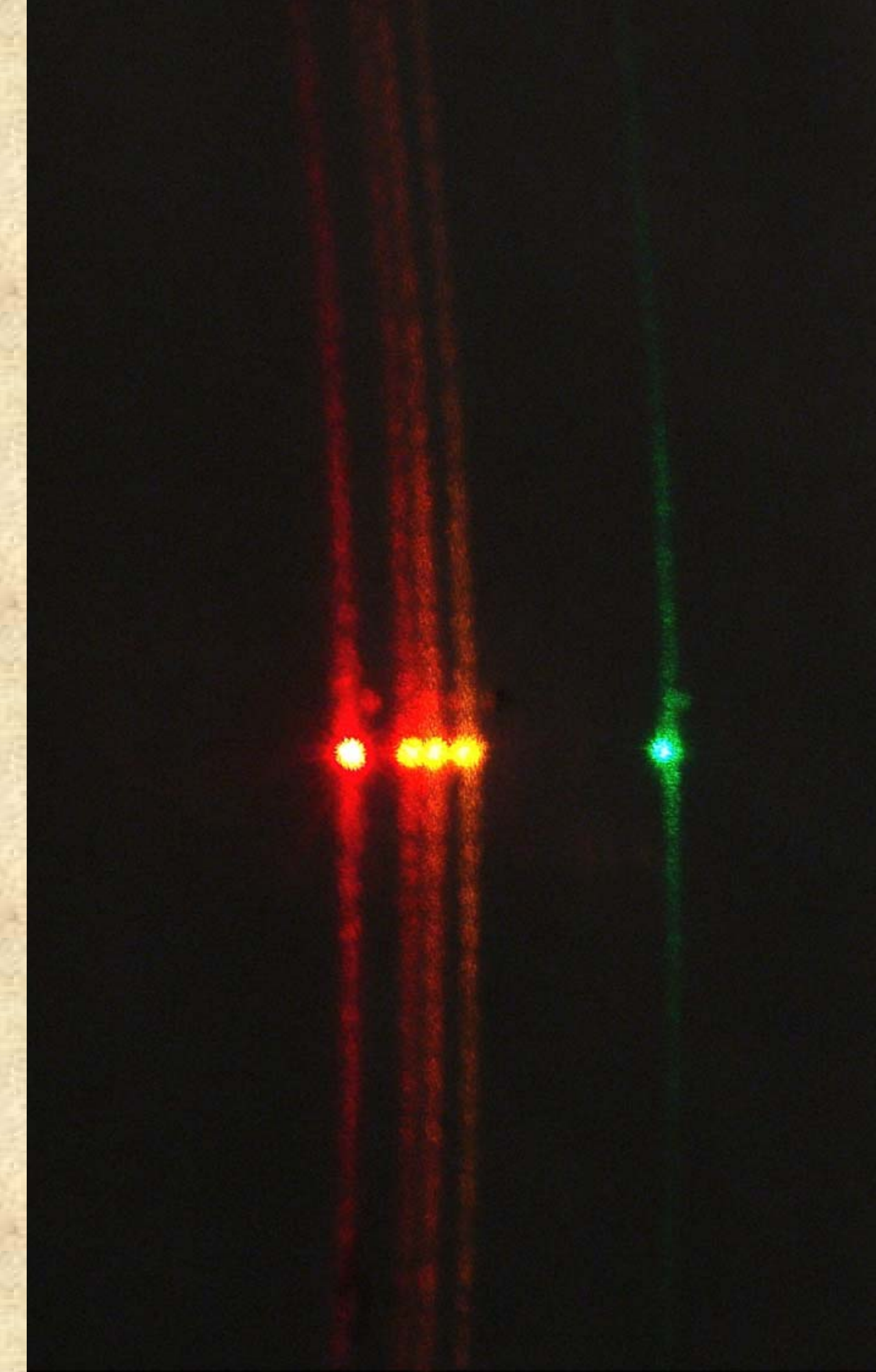

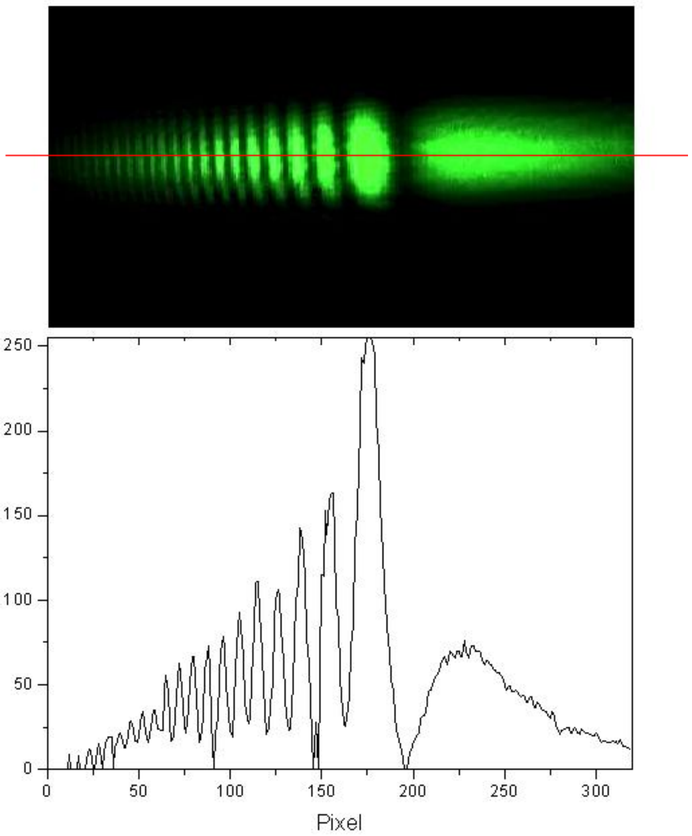

Medidor de vácuo

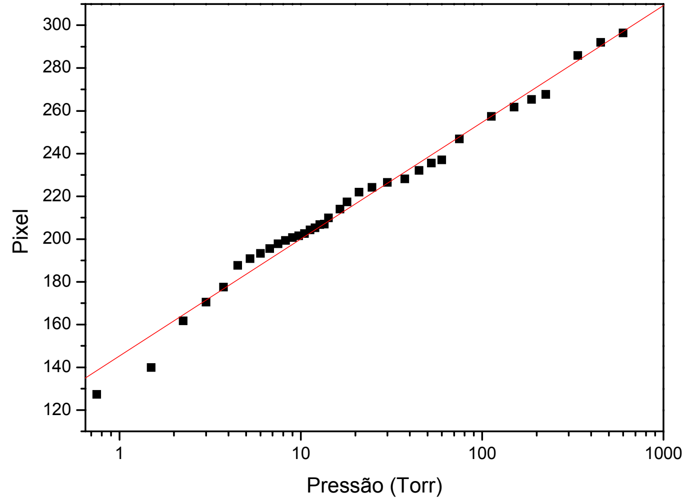

Medidor de umidade

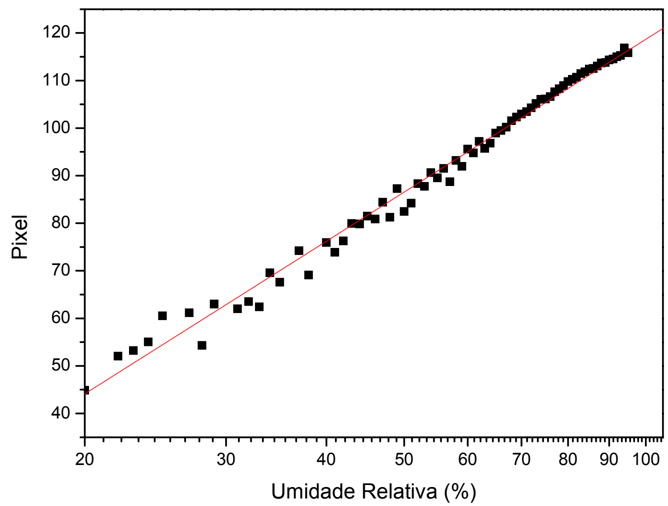

$$E_i(x_i, y_i, 0) = \exp\left(-\frac{y_i^2}{w_0^2}\right) \int_{-\infty}^{+\infty} \hat{E}_i(\sigma) \exp(2j\pi\sigma x_i)\, d\sigma$$

$$\sigma = \sin(\theta)/\lambda_0$$

$$\hat{E}_i(\sigma) = E_0\sqrt{\pi}\, w_0 \exp(-\pi^2 w_0^2 \sigma^2).$$

$$\mu = \cos(\theta)/\lambda_0.$$

$$E_r(x_r, y_r, z_r) = \exp\left(-\frac{y_r^2}{w_0^2}\right) \int_{-\infty}^{+\infty} \hat{E}_i(\sigma) f(\sigma) \times \exp(2j\pi\sigma x_r) \exp(2j\pi\mu z_r)\, d\sigma$$

$$f(\sigma) = t_1(\sigma) t_2(\sigma) r(\sigma) \exp(j\Delta\phi_p(\sigma))$$

$$E_r(x_r, y_r, z_r) = \exp\left(-\frac{y_r^2}{w_0^2}\right) \int_{-\infty}^{+\infty} F(\sigma, x_r) \times \exp(2j\pi\sigma x_r)\, d\sigma$$

$$F(\sigma, z_r) = \hat{E}_i(\sigma) f(\sigma) \exp(jk_0 z_r) \exp(-j\pi\sigma^2 z_r)$$

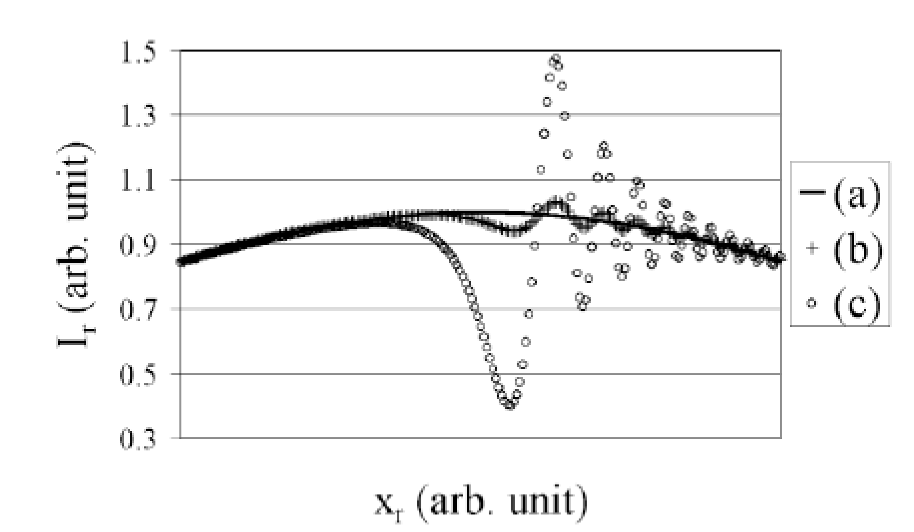

3) Óptica não linear – franjas de Maker (SHG)

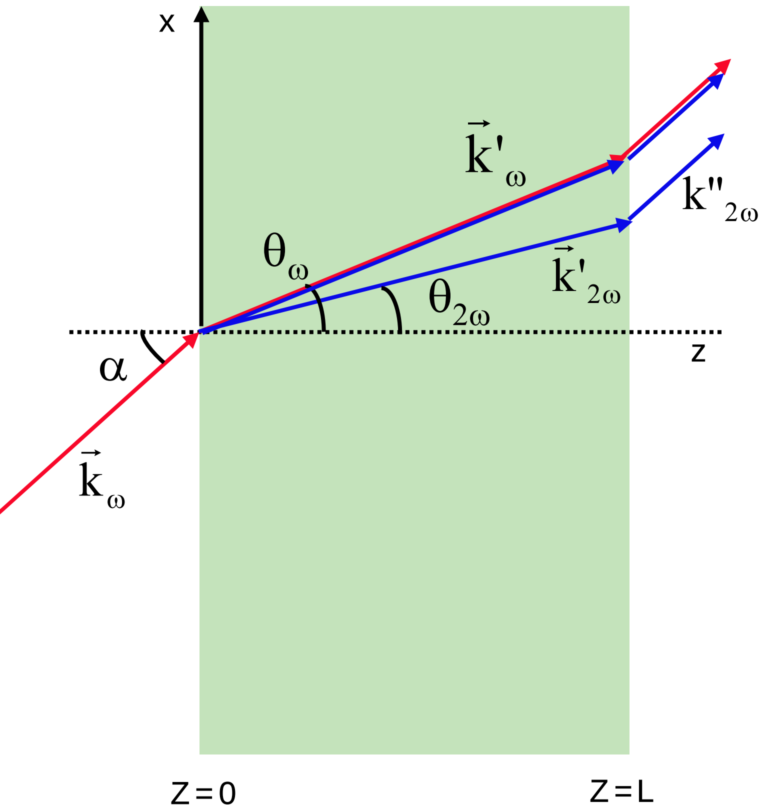

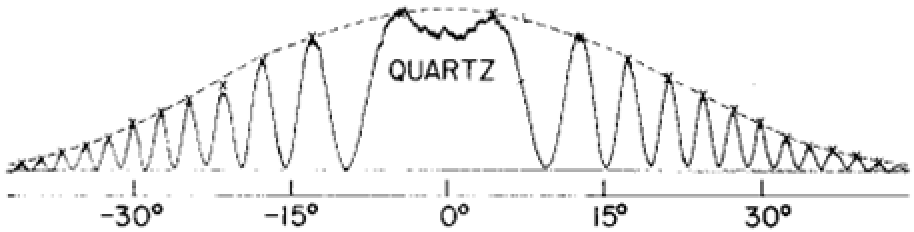

$$\mathbf{E}_{2\omega}' = \hat{e}_f\, E_f' \exp(i\mathbf{k}_f \cdot \mathbf{r}) + \hat{e}_b\left[4\pi \mathcal{P}_{2\omega}' / (n_\omega^2 - n_{2\omega}^2)\right] \times \exp(i\mathbf{k}_b \cdot \mathbf{r})$$

$$I^{2\omega} \propto \left|\frac{\chi^{(2)}}{\Delta\varepsilon}\right|^2 \left|I^{\omega}\right|^2 A\left(t_{12}^{\omega}\right)^4 \sin^2\left[\frac{2\pi\left(n_2^{\omega}\cos\theta_2^{\omega} - n_2^{2\omega}\cos\theta_2^{2\omega}\right)L}{\lambda}\right]$$

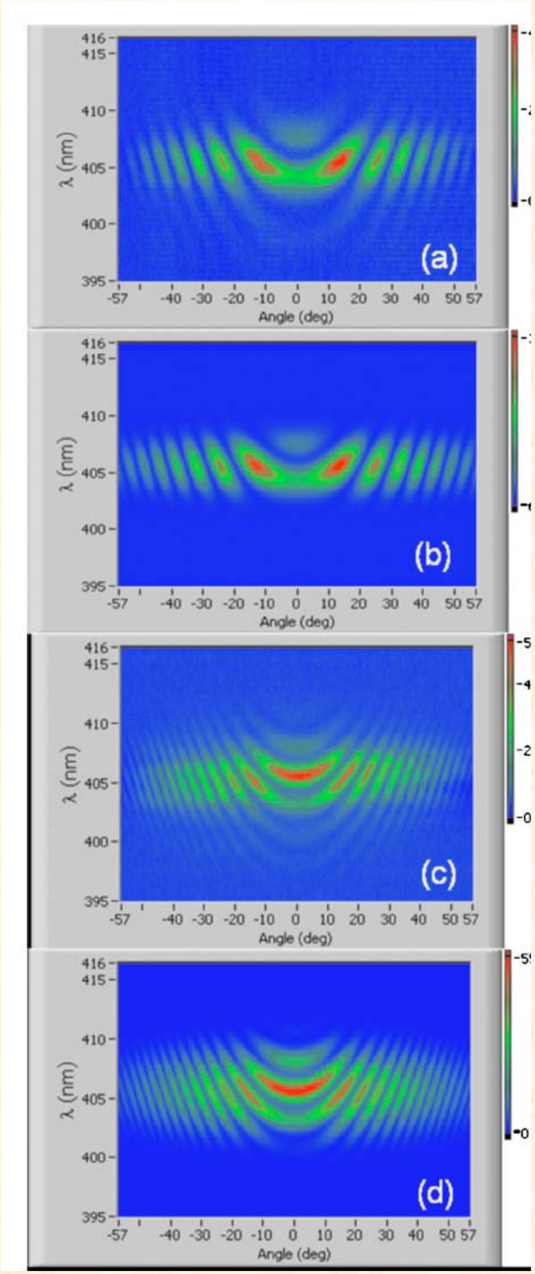

$$I^{3\omega} \propto \left|\frac{\chi^{(3)}}{\Delta\varepsilon}\right|^2 \left|G(\omega)\right|^2 f(\theta_1)A^2\left(t_{12}^{\omega}\right)^6 \sin^2\left[\frac{3\pi\left(n_2^{\omega}\cos\theta_2^{\omega} - n_2^{3\omega}\cos\theta_2^{3\omega}\right)\ell}{\lambda}\right]$$

$$G(\omega) = \int\int E(3\omega - \omega_2 - \omega_3)E(\omega_2)E(\omega_3)\,d\omega_2 d\omega_3$$

$$t_{12}^{\omega} = \frac{2n_1\cos\theta_1}{n_1\cos\theta_1 + n_2^{\omega}\cos\theta_2^{\omega}}$$

$$A = \frac{n_2^{3\omega}\cos\theta_2^{3\omega} + n_2^{\omega}\cos\theta_2^{\omega}}{n_2^{3\omega}\cos\theta_2^{3\omega} + n_1^{3\omega}\cos\theta_1^{3\omega}}$$

Determina-se $\chi^{(3)}$ por comparação com a silica e os coeficientes de Sellmeier através do fitting das franjas com algorítmo genético

$$\Phi = \frac{3\pi\left(n_2^{\omega}\cos\theta_2^{\omega} - n_2^{3\omega}\cos\theta_2^{3\omega}\right)\ell}{\lambda} \cong \frac{\pi}{\lambda^{TH}}\frac{\left(n_2^{3\omega} - n_2^{\omega}\right)}{\cos\theta_2^{\omega}}\ell = m\pi$$

$$m\lambda_m^{TH} = \frac{\left(n_2^{3\omega} - n_2^{\omega}\right)}{\cos\theta_2^{\omega}}\ell \cong \left(n_2^{3\omega} - n_2^{\omega}\right)\ell\left(1 + \frac{1}{(n_2^{\omega})^2}(1-\cos\alpha)\right)$$

$$m\lambda_m^{TH} \cong \Delta n(\lambda_m^{TH})\;\ell\left(1+\frac{1}{(n_2^{\omega})^2}(1-\cos\alpha)\right)$$

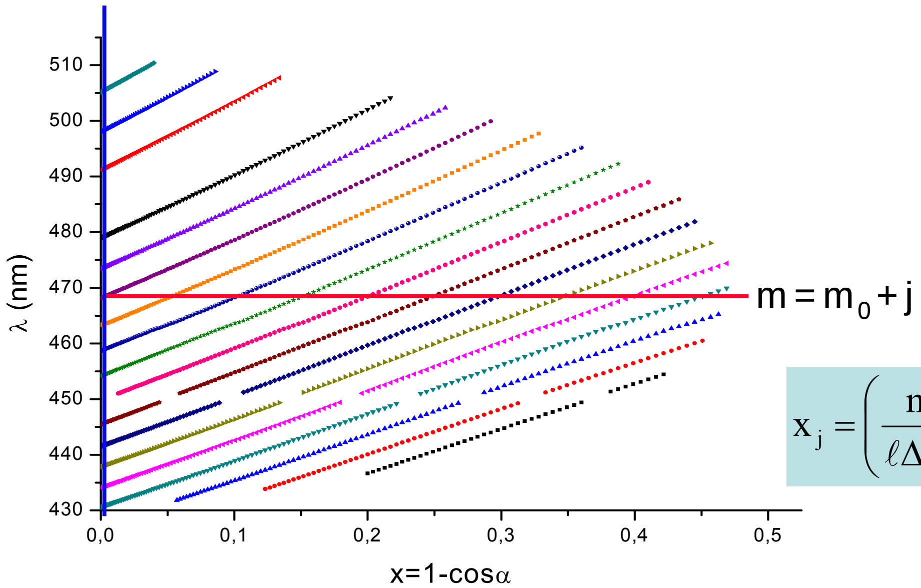

$$x_j = \left(\frac{m_0\lambda_m^0}{\ell\Delta n(\lambda_m^0)}-1\right)n^2 + \frac{\lambda_m^0}{\ell\Delta n(\lambda_m^0)}\,j = A + Bj$$

$$m\lambda_m^0 = \ell\Delta n(\lambda_m^0) \Rightarrow m = \frac{\ell\Delta n(\lambda_m^0)}{\lambda_m^0} = \frac{n^2(\lambda_m^0)}{B}$$

$$\frac{1}{B(\lambda_m^0)} = \frac{m_0}{n^2(\lambda_m^0)} + \frac{j}{n^2(\lambda_m^0)}$$